DOI: 10.5604/01.3001.0053.8686
Volume 119 • Issue 1 • July 2023
Journal of Achievements in Materials and Manufacturing Engineering
International Scientific Journal published monthly by the World Academy of Materials and Manufacturing Engineering

Influence of the base metal grain size and heat input on decarburization in single pass SAW and multi pass SMAW welded joints of dissimilar ferritic steels

M.O. Nimko*, V.Yu. Skulskyi
E.O. Paton Electric Welding Institute NASU, 11 Malevich St., Kiev 03680, Ukraine
* Corresponding e-mail address: maxim.nimko@gmail.com
ORCID identifier: https://orcid.org/0000-0002-9672-4921 (M.O.N.)

ABSTRACT

Purpose: This paper aims to assess a separate influence of heat input and base metal grain size on microstructural evolution in the weld adjacent zone of bainitic steels with 1.5…2.0% Cr, welded or overlayed with consumables with 9% Cr after post-weld heat treatment.

Design/methodology/approach: Analysis of the width of decarburised layer on microphotographs of welded or overlayed specimens after tempering at 750°C. Specimens were made by using different welding approaches: single-pass welding, multi-pass welding and overlaying.

Findings: It is shown that with an increase of the heat input energy, the width of the resulting decarbonised layer decreases linearly; the increase of the base metal grain size leads to a decrease in the layer width after tempering at 750°C. The microhardness testing showed the average hardness in the decarburised layer of 15Kh2M2FBS steel was 161 HV0.1 (minimum – 154 HV0.1), while the average hardness in the rest of the heat-affected zone was 192 HV0.1.

Research limitations/implications: Future research may include comparing the creep rupture strength of the weldments made with different welding parameters or base metal grain size to assess the influence of these factors on creep rupture strength.

Practical implications: Results permit to achieve minimisation of the rate of carbon diffusion in the weld-adjacent area of the heat-affected zone by means of variation of welded parameters and base metal grain size.

Originality/value: An influence of high-diffusivity paths (grain boundaries) on carbon diffusion in the heat-affected zone of dissimilar weldments was confirmed experimentally; the correlation between base metal grain size/welding parameters and the rate of the diffusion during high-temperature exposure was found.

Keywords: Welding, Dissimilar welds, Carbon diffusion, Grain boundaries

Reference to this paper should be given in the following way:

M.O. Nimko, V.Yu. Skulskyi, Influence of the base metal grain size and heat input on decarburization in single pass SAW and multi pass SMAW welded joints of dissimilar ferritic steels, Journal of Achievements in Materials and Manufacturing Engineering 119/1 (2023) 14-26. DOI: https://doi.org/10.5604/01.3001.0053.8686

MANUFACTURING AND PROCESSING

© Copyright by International OCSCO World Press. All rights reserved. 2023

1. Introduction

The main thermodynamic cycle of thermal power plants, used in modern thermal power generation, is the Rankine cycle with superheated steam. To implement this thermal cycle, different sections of the steam-water circuit at a power plant must have different temperature and pressure parameters of the working fluid. In order to make the construction of the power plant cheaper, sections with lower steam parameters are made of low-alloyed bainitic steels with 0.5-2.25% Cr (water wall tubes, operating at temperatures of 550-580°C) and martensitic steels with 9-12% Cr (upper sections of water wall tubes, headers, main steam pipelines) for temperatures up to 625-630°C. Sections with higher steam parameters are made of more expensive austenitic steels (superheater and reheater tubes, operating at temperatures up to 660-680°C) [1]. To implement a closed steam-water circuit, these areas are combined by welding, forming joints of dissimilar steels. Thousands of welded joints between low-alloyed and high-alloyed ferritic steels can be found in a modern power plant, in particular, in welds between upper and lower sections of water wall panels, in cases of replacing old headers with headers made of new steels, in sections of welded rotors, etc. [2].

Due to carbon migration a decarburised layer with reduced hardness appears in such joints on the side of less alloyed steel during heat treatment or high-temperature service [2,3]. Chromium and some other carbide-forming elements are known to lower the chemical potential of carbon in the steel, thus promoting the diffusion of carbon from less alloyed steel to a more alloyed one with higher chromium content [3]. At the same time, it is possible to observe the diffusion of carbon from areas with a lower concentration of carbon to areas with a higher concentration, even in a single-phase metal.

The effect of the decarburised layer on the long-term strength of the joint has been the subject of debate for many years. Most authors believe that the layer has a noticeable effect on the mechanical properties of joints [4-9]. In particular, it was noted that:

- carbon migration significantly reduces the nano-hardness and yield strength of the decarburised layer, which becomes the weakest area in the entire joint [10];
- with an increase in the operating temperature, the probability of failure in the area of the decarburized layer during high-cycle fatigue increases [11, 12];
- the decarburised layer significantly reduces the creep life of the weld at high stress levels; however, when the stress level drops, this effect becomes less noticeable [13].

Under service conditions, two main types of creep damage accumulation can occur in welded joints between low-alloyed and high-alloyed ferritic steels. One mechanism prevails for a longer time of failure at lower loads, the other for shorter failure time and higher loads. The first process refers to type IV cracking and is characterised by weakening, accumulation of damage and crack initiation in the fine-grained heat affected zone (FGHAZ) and the inter critically heated region of the heat affected zone (ICHAZ) [14]. The second process – type IIIa crack formation – is characterised by large local stresses and by accumulation of damage in the decarburised layer in the heat-affected zone (HAZ) near the fusion line [2,4]. Statistical data on cracks detected during the inspection of power plants in Great Britain showed that a significant number of defects (21% of all damaged joints) were of type IIIa, and the main reason for this was the diffusion of carbon from low-alloyed steels to high-alloyed steels in dissimilar joints [15].

However, in some works, no influence of the decarburised layer on failure during mechanical tests was noted [16,17].

Also, a carburised layer is formed in more alloyed steel. It was shown [18,19] that microcracks can originate in the hard carbonised layer. Such micro defects mainly originate in the transition zone and have an intergranular character. Some authors [20,21] pointed out that the critical factor for the failures from carbon depleted zones is the interaction between adjacent carburised and decarburised areas, which provides extreme physical and chemical heterogeneity across a narrow distance: microcracks originate in the carburised zone and the presence of an adjacent decarburized layer aids in crack propagation under stress.

To overcome the problem of carbon diffusion in the joints of dissimilar steels, it was proposed to use nickel-based welding materials, which have a low carbon diffusion coefficient and thus prevent its migration from the ferritic steel into the weld. However, since traditional nickel-based materials (Alloy 82/182/617/625, etc.) contain a large number of carbide-forming elements (Cr, Mo, Nb, Ti), their ability to restrain carbon diffusion effectively is debatable [22-24].

According to existing data [25], grain size could be considered as one of the physical factors which affects the rate of carbon loss of parent metal. The effect is stronger in microstructure with smaller grains. Heat input could produce an additional influence on the rate of development of decarburized layer: it was shown [26] that in the case of dissimilar weldments between martensitic (P91) and austenitic steels, higher heat input leads to a lower rate of decarburisation in the HAZ of P91 steel.

The work aims to study the influence of the base metal grain size and the welding heat input on the size of the decarburised layer in the dissimilar welded joints of ferritic steels after heat treatment. 15Kh1M1F, 15Kh2M2FBS steels and filler materials with 9% Cr were used as low- and high-alloyed components of the joints. 15Kh2M2FBS steel ($R_{p0.2}$ = 628.8 MPa, R_m = 750.0 MPa, A = 16.7%) is used for the manufacture of turbine casings; it can be found in joints of dissimilar steels when the turbine casing is connected with a main steam pipeline made of P91 steel; 15Kh1M1F steel ($R_{p0.2}$ = 447.8 MPa, R_m = 607.4 MPa, A = 17.4%) is used for manufacturing the rims of turbine diaphragms, to which turbine blades, made of steel with 12% Cr, can be welded.

2. Experimental procedure and results

The following approaches were used to obtain experimental combinations and to model structural heterogeneity:

1) single pass SAW welding of 15Kh2M2FBS steel using wire with 9% Cr. The base metal sides of the joint differed in the grain size: one side of the joint, which was welded in the delivery condition, had a fine-grained structure (grain size index G = 9 according to EN ISO 643); the other side of the joint was subjected to preliminary heat treatment at 1200°C, 30 min (cooling in air) + 730°C, three h to obtain a coarse-grained structure (G = 4). The sides were then welded using Thermanit MTS 3 wire (ø2.4 mm) under Böhler Marathon 543 flux; welding parameters I = 360-380 A, U = 34.4 V, V = 20.7 m/h (Fig. 1a).

The idea of this experiment and the next one was to examine pieces with different grain sizes, which were welded with identical thermal and welding parameters.

To develop structural heterogeneity after welding, tempering was performed at a temperature of 750°C for 3 and 18 h.

2) multi-pass welding of 15Kh2M2FBS and 15Kh1M1F steels using electrodes with 9% Cr; the sides of the joints differed in the size of the base metal grains:
   - in the weldment of 15Kh2M2FBS steel, one side – delivery condition, G = 7; second side – G = 3 after heat treatment (1200°C, 30 min + 740°C, 2.5 h).
   - in the weldment of 15Kh1M1F steel, one side – delivery condition, G = 10; second side – G = 1 after heat treatment (1200°C, 30 min + 740°C, 2.5 h).

The joints were welded using Thermanit Chromo 9V electrodes (ø3.2 mm): I = 115...120 A, U = 24 V; preheat and interpass temperatures were ~200...250°C (Fig. 1b).

After welding, heat treatment was performed at 750°C for 6 and 12 hours.

3) overlaying with 9% Cr metal onto 15Kh2M2FBS steel using Thermanit Chromo 9V electrodes. Two layers with 3-4 beads in each layer were deposited on a plate with a thickness of 30 mm (Fig. 1c). The overlaying parameters were varied to assess the heat input influence on the rate of carbon depletion in the HAZ. Heat input (heat input per unit length of weld) HI was calculated using the formula:

$$HI = \frac{\eta \cdot I \cdot U}{V} \quad (1)$$

where η is the efficiency of the welding method (took η = 0.85); I – current strength, A; U – arc voltage, V (took U ≈ 24 V); V – welding speed, m/s.

Such two-layer depositions were made to simulate the thermal effect on the base metal in the conditions of multilayer welding.

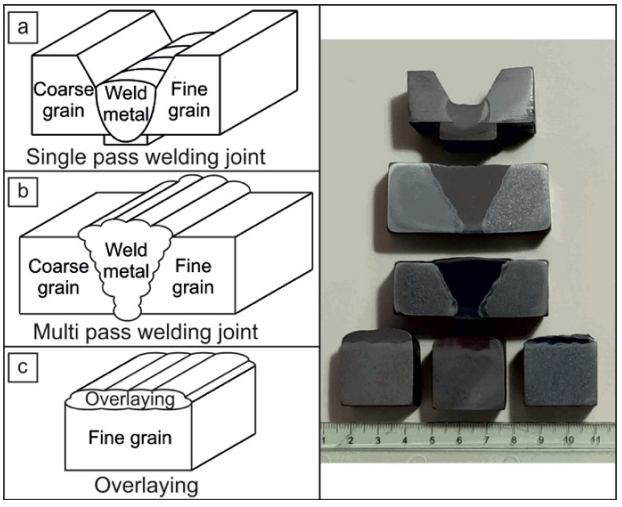

Fig. 1. Schemes of single/multi-pass welded joints with different grain size sides and overlayed plates

After surfacing, heat treatment was carried out at 750°C for 6 and 12 h.

Actual HI values for three different parameters of overlaying are shown in Table 1. For the first overlaying mode (I = 135-140 A, V ≈ 4.6×10^{-3} m/s) the average heat input of the first layer was 613 kJ/m; for the second mode (I = 100-105 A, V ≈ 3.3×10^{-3} m/s) – 648 kJ/m, for the third overlaying mode (I = 100-105 A, V ≈ 7.2×10^{-3} m/s) – 291 kJ/m.

All metallographic sections, produced in the above experiments were etched using a 5% HNO_3 solution (5 ml HNO_3, 95 ml ethyl alcohol, 1 g picric acid).

Table 1.
Parameters of overlaying

Welding current, A	Layer 1 (directly overlaid on base metal)		Layer 2 (additional, overlaid on layer 1)	
	Welding speed, $\times 10^{-3}$ m/s	Heat input, kJ/m	Welding speed, $\times 10^{-3}$ m/s	Heat input, kJ/m
135-140	4.7	599	4.5	626
	4.4	640	3.4	828
	4.7	599	4.9	575
100-105	2.9	725	3.5	600
	3.4	618	2.9	725
	3.5	600	3.3	637
100-105	7.8	269	8.2	256
	7.1	296	7.2	291
	7.0	300	7.3	288
	7.0	300	7.8	269

Table 2.
Chemical composition of steels and welding materials

Steel grade/filler material	Chemical composition, wt. %								
	C	Si	Mn	Cr	Ni	Mo	V	Nb	Others
15Kh2M2FBS	0.115	0.468	0.67	1.95	0.16	1.12	0.32	0.072	Cu 0.15
15Kh1M1F	0.154	0.40	0.88	1.52	0.10	1.04	0.4	-	-
Thermanit MTS 3	0.1	0.3	0.5	9.0	0.7	1.0	0.2	-	-
Thermanit Chromo 9V	0.09	0.2	0.6	9.0	0.8	1.1	0.2	0.05	N 0.04

The chemical composition of steels and filler materials used in the study is shown in Table 2. The use of filler materials with 9% Cr is consistent with practical recommendations, because welded joints with stronger weld metal provide a longer creep life of weldments than joints with weaker weld metal (as in the case of use of filler materials with 2.25% Cr) [16,27,28].

2.1. The results of experiments and their analysis

The main preliminary objective for experiment No. 1 was to determine the width of the decarburised layer in the weld-adjacent zone of HAZ in steels with different grain sizes. The single run welding was chosen as the one, which can produce empirically pure results, unaffected by the influence of redeposition and reheating from additional runs.

In a single pass joint of 15Kh2M2FBS steel with different grain sizes after tempering at 750°C for 18 h, the formation of a wide ferrite layer with reduced hardness was observed in the area away from the fusion line on the side with a small grain size (Fig. 2). In contrast, such a layer was not observed on the side with large grain size. It should be noted that after tempering at 750°C for three h, no such layers were observed on the side of the weld with small grains. The ferrite layer is formed approximately in the fine-grained area and in the heated area of the HAZ.

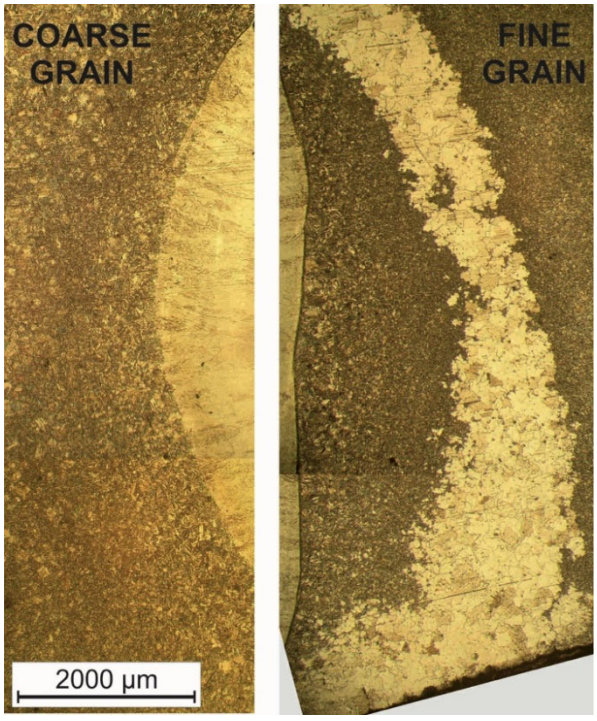

Fig. 2. Panoramic microstructure of the HAZ of a single pass weldment of 15Kh2M2FBS steel with large (G=4) and small (G=9) initial grain sizes after tempering at 750°C, 18 h (magnification x25)

Measurements of microhardness on both sides of the joint also show that in the HAZ of small grain base metal, the corresponding weakening is more noticeable; the hardness significantly decreases in the area with a ferrite structure (Fig. 3). The microhardness testing showed the average hardness in the decarburised layer of 15Kh2M2FBS steel was 161 HV0,1, the lowest hardness in this layer – 154 HV0,1; the average hardness in the rest of the fine-grained side of HAZ was 192 HV0,1. The average hardness in the HAZ of the coarse-grained side of the weld was 210 HV0,1.

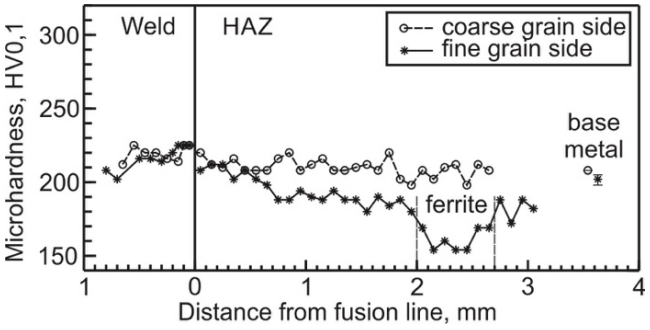

Fig. 3. Measurement of microhardness in a single pass weldment of 15Kh2M2FBS steel with different grain sizes in the state after tempering at 750°C, 18 h

After the objective for the experiment No. 1 was not achieved, it was decided to repeat the experiment with multi-pass weldments.

To quantitatively assess the influence of grain size in multi-pass welded joints (experiment No. 2) after tempering at 750°C for 6 and 12 h, metallographic sections were made from the joints and panoramic micrographs of the HAZ near the fusion line (with 4-5 micrographs, depending on the thickness of the welded plates) were obtained for each type of weldments using an optical microscope with magnification x25 (Fig. 4). Microstructure data were obtained using the free ImageJ software [29]: ferrite areas were converted into a black-and-white mask (Fig. 5), and the area of the black-painted ferrite layer was estimated using the "Histogram" tool in the ImageJ software; also additionally the length of the fusion line was measured on each photomicrograph using the "Measure" tool.

The idea of overlaying in experiment No. 3 was to imitate multi-pass welding with different welding parameters on a base plate.

Analogous panoramic images were obtained for overlaying on 15Kh2M2FBS steel. After tempering at 750°C, 6 h, no development of ferrite layers was observed in the samples deposited with a heat input of ~600 kJ/m; however, in the sample deposited with HI ≈ 291 kJ/m, the formation of ferrite microconstituents was observed in the weld adjacent HAZ between weld beads (Fig. 6).

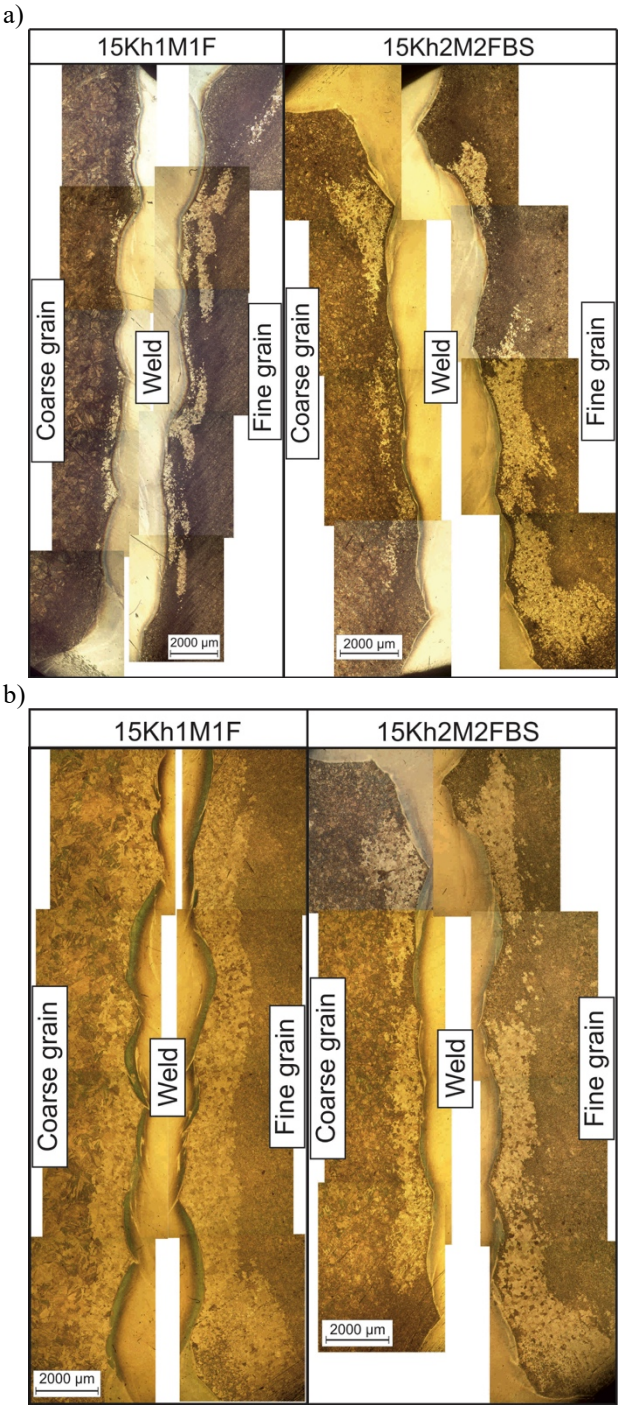

Fig. 4. Panoramic micrographs of the HAZ of welded joints made of 15Kh1M1F and 15Kh2M2FBS steels after tempering at (a) 750°C, six h and (b) 750°C, 12 h (magnification x25)

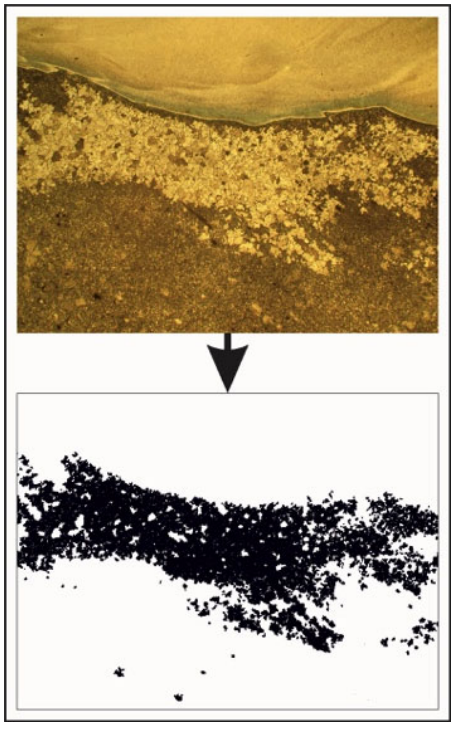

Fig. 5. An example of converting a photomicrograph with a decarburized ferrite area into a black-and-white mask

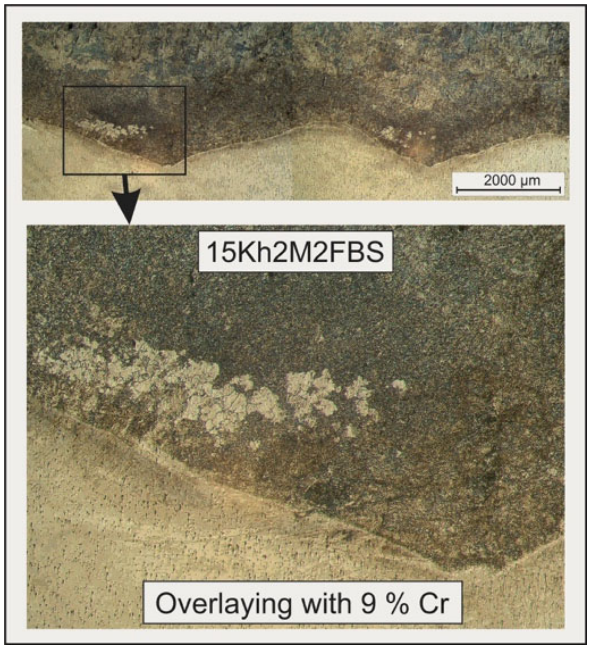

Fig. 6. Development of a decarburised layer in the HAZ of 15Kh2M2FBS steel, made with overlaying I = 100-105 A, V ≈ 7.2 mm/s, after tempering at 750°C, 6 h (magnification x25 for the panoramic image and x63 for the bottom image)

After tempering at 750°C, 12 h, the formation of ferrite areas in the HAZ of 15Kh2M2FBS steel near the fusion line is observed in all samples. Fragments of panoramic micrographs are shown in Figure 7.

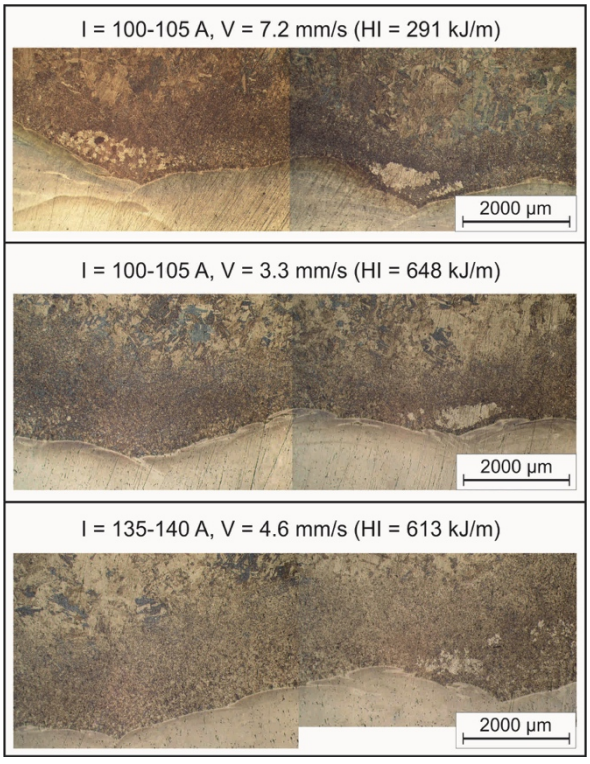

Fig. 7. Examples of panoramic images of HAZ of 15Kh2M2FBS steel after tempering at 750°C, 12 h (magnification of single images x25)

To estimate the amount of decarburisation, the concept of the specific width of the decarburized (ferrite) surface S was introduced, which was defined as the fraction of the division of the total area of the decarburised zones A by the total length of the fusion line L:

$$S = \frac{A}{L} \tag{2}$$

Conditionally, this concept corresponds to the concept of the average width of the decarburised layer (Fig. 8), which can be used to determine decarburisation, for example, in dissimilar welds of martensitic and austenitic steels [26], in which the decarburised layer develops uniformly from the fusion line during high-temperature exposure. However, it was noticed that in low-alloyed bainitic steels, such as 15Kh1M1F or 15Kh2M2FBS, decarburisation during tempering develops differently and is accompanied by the formation of ferrite areas of uneven width (Fig. 4, Fig. 9),

which approximately develop along the fine-grained zones of FGHAZ and ICHAZ from repeated welding beads and can develop at a certain distance from the fusion line, with an unaffected (by diffusion) zone between fusion line and decarburised ferritic microconstituents (Fig. 9) [30]. Therefore, a similar concept of the specific width of the decarburised layer was introduced.

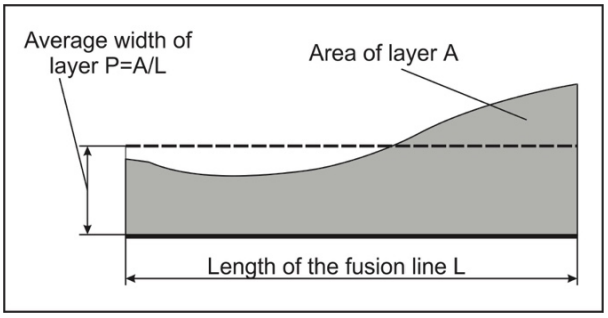

Fig. 8. Determination of the average width of the layer

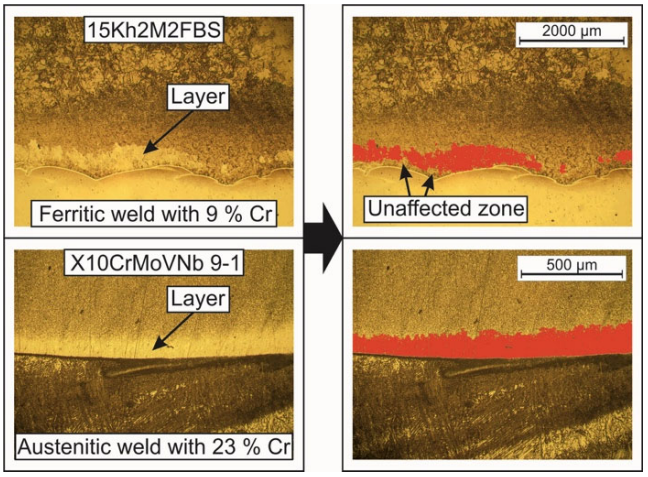

Fig. 9. Comparison of the modes of decarburisation development in low-alloyed bainitic 15Kh2M2FBS steel after tempering at 750°C, 8 h (magnification x25) and martensitic X10CrMoVNb 9-1 (P91) steel after tempering at 760°C, two h + 700°C, 14 h (magnification x100)

The results of measurements of the specific width of decarburisation for joints of 15Kh2M2FBS and 15Kh1M1F steels depending on the grain size (index) and duration of exposure at a temperature of 750°C are shown in Figure 10. There is a trend, observed separately for each steel grade on the graph: with an increase in the grain index (correspondingly, with a decrease in the average diameter of the grains), the specific width of the decarburised layer increases. After exposure for 6 hours, 15Kh2M2FBS and 15Kh1M1F steels had different decarburisation kinetics, which is reflected by different angles of inclination of the corresponding graphs of the change in the width of the decarburised layer depending on the grain size: $\alpha_1 > \alpha_2$ in Figure 10.

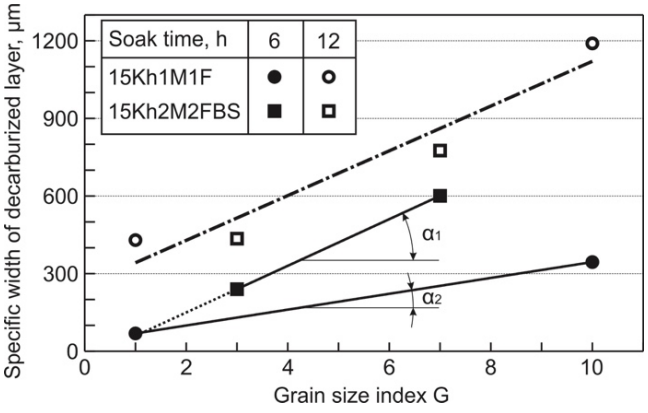

Fig. 10. Dependencies of the specific width of the decarburised layer on the grain size of the base metal after tempering at 750°C

After exposure for 12 hours, the value of the specific width of the decarburised layer, depending on the grain size index for both sheets of steel, begins to correspond to the same linear law. The dash-dotted line on the graph is constructed by the hour least squares method, taking into account all values for both sheets of steel after exposure at 750°C for 12 hours.

It is known that the dependence of the width of a diffusion layer on the duration of exposure at a constant temperature agrees with the inverse parabolic law $L = a \cdot \sqrt{t}$ [31]. However, as the experiments showed for the two studied sheets of steel, this law of change in the width of the decarburised layer L differs, probably, due to the peculiarities of the microstructure. Thus, for 15Kh1M1F steel, the experimental values are more consistent with the parabolic law$L = a \cdot t^2$ (Fig. 11a, black colour lines; the interpolation line according to the law$L = a \cdot \sqrt{t}$ is shown in grey colour for comparison), and for steel 15Kh2M2FBS – with the law $L = a \cdot \sqrt{t}$ (Fig. 11b).

In Figure 12, the dependence of the specific width of the decarburised layer on the overlaying heat input energy is presented. It is shown that an increase in the heat input from 300 to ~600 kJ/m leads to a noticeable decrease in the width of the decarburised zone after the same heat treatment, which may be explained by grain coarsening in the weld-adjacent zone of the HAZ (see Discussion section).

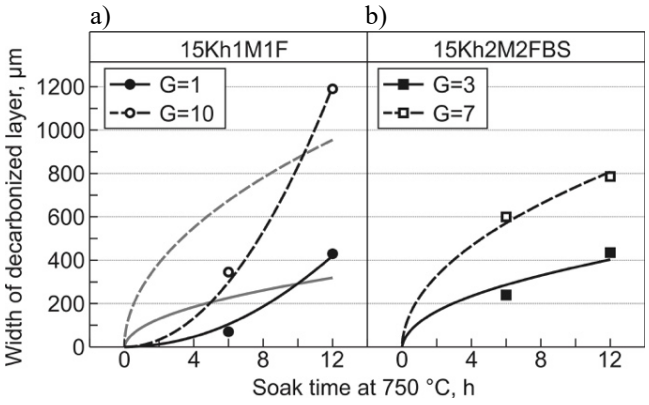

Fig. 11. Dependencies of the specific width of the decarburised layer on the grain size and the soak time at a temperature of 750°C

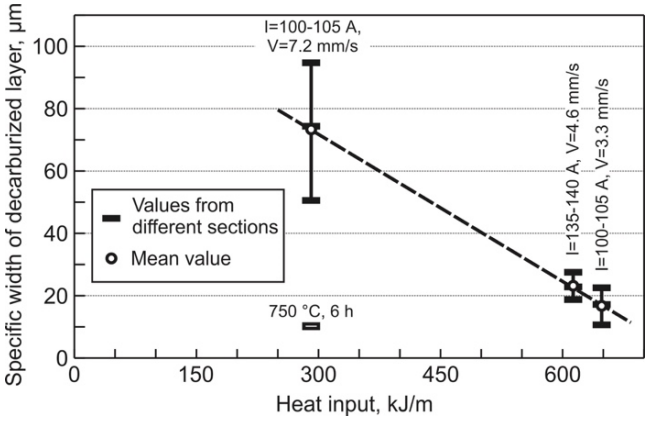

Fig. 12. Dependence of the specific width of the decarburized layer on the heat input of overlaying in the HAZ of 15Kh2M2FBS steel after tempering at 750°C, 12 h

Similar values of the decarburised layer width for welding modes 1) I = 135-140 A, V ≈ 4.6×10^{-3} m/s and 2) I = 100-105 A, V ≈ 3.3×10^{-3} m/s (having similar values of heat input energy ~ 600 J/m and different values of current strength and welding speed) indicate that heat input energy is a decisive factor in determining the width of the decarburized layer after welding and heat treatment.

2.2. Discussion

Polycrystalline bodies, such as real steels, contain several extended defects, including dislocations, grain boundaries, pores, and surfaces. The diffusion coefficient D in the crystal lattice or the above-mentioned defects of the material depend on the degree of freedom that the diffusing atom receives in a certain location in the material. Diffusion through the lattice represents the most serious limitation for atomic migration due to its close packing. Dislocations, as extended defects in the lattice, restrict atomic movement in the direction of the dislocation line less than the lattice. High-angle grain boundaries, with their less densely packed structure, contribute to fast atomic diffusion and surfaces offer the least constraints to the motion of diffusing atoms [32].

In most cases, the following ratio of the values of the diffusion coefficients is realised in the metal body:

$$D_{lattice} << D_{dislocation} \leq D_{grain\ boundary} \leq D_{surface}$$

Diffusion through defect sites becomes more important at low temperatures. For example, grain boundary diffusion in polycrystalline materials plays a major role at temperatures below $0.6\cdot T_{melting}$ [32].

While diffusion through regions with defects may occur faster than diffusion through a defect-free bulk of the material, the overall influence of this effect depends on the relative number (density) of extended defects in the solid. A decrease in the diffusion rate can be achieved by increasing the size (diameter) of grains, which leads to a decrease in the total area of grain boundaries per volume unit. At temperatures of heat treatment and high-temperature service in thermal power plants, diffusion through defects (grain boundaries, dislocations) is of primary importance. Under these conditions, a decrease in the area of grain boundaries leads to a significant decrease in the flow of diffusing atoms.

During welding, as a result of the effect of the thermal cycle from the arc, zones with different grain sizes are formed in the HAZ, which correspond to changes in diffusion "resistance" of the HAZ (Fig. 13).

Each zone is represented by its characteristic microstructure and properties [14]:

- *Grain growth zone*: this zone adjacent to the fusion line experiences temperatures well above the A_{C3} transformation temperature. Any precipitates obstructing the growth of austenite grains at lower temperatures dissolve, resulting in coarse grains of austenite, forming a bainitic/martensitic microstructure on cooling in lower chromium steels. The coarse-grained zone (CGHAZ) features the highest hardness of the HAZ and generally, low toughness values are expected.
- *Grain refined zone*: lower peak temperatures of about 1100°C, just above A_{C3}, result in an improper development of austenite producing small austenitic grains (FGHAZ). In addition, the peak temperature may not be high enough to dissolve precipitates completely, limiting the grain growth by pinning the austenite grain boundaries. The fine grained region of the HAZ is

regarded as the weakest link in weldments during creep-loaded service. At longer service times and lower stress levels, most of the weldments of creep-resistant ferritic steels fail within this region by the so-called type IV mechanism.

- *Partially transformed zone – inter critical HAZ*: peak temperatures between A_{C1} and A_{C3} transformation temperatures result in a partial transformation of α into γ on heating. Partial dissolution of precipitates may be experienced in this part of the HAZ, and coarsening of undissolved precipitates can occur, especially during subsequent PWHT. After cooling, a twofold microstructure consisting of newly formed bainite (for low chromium steels) and the tempered original microstructure coexist. The inter critical HAZ shows a small grain size and exhibits the lowest hardness values in weldments. This sub-zone of the HAZ shows similar susceptibility to type IV cracking as the grain refined zone.
- *Over-tempered region*: with peak temperatures experienced below Ac1, the microstructure does not undergo any phase transformations. However, the original microstructure is locally tempered at higher temperatures than the annealed base material. As a result, coarsening of precipitates may be enhanced by a higher diffusion coefficient at this temperature.
- *Zone of unchanged base material*: the zone of unchanged base materials concerns temperatures up to circa 700°C, in which changes in the morphology of constituents do not appear to occur.

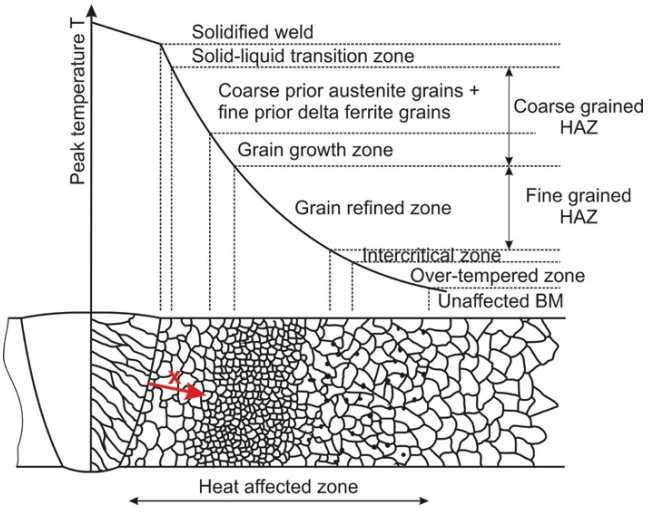

Fig. 13. The scheme of the distribution of subsections in the HAZ of a welded joint depending on the temperature of the thermal cycle of welding [14]

Bearing in mind the above theses, the obtained results can be explained as follows.

In a single pass welded joint (experiment No. 1), the role of a diffusion intensifier is performed by the top and bottom surfaces of the side plates, which have a higher diffusion coefficient $D_{surface}$. Where intensive decarburisation occurs during tempering due to oxidation in the furnace atmosphere (in these areas, there is a fluctuation in the width of the ferrite layer – it becomes wider above and below in the joint, near the side surfaces), and decarburisation, which develops along the fine-grained zone of FGHAZ and ICHAZ, is far from the weld metal. Kinetics of ferrite interlayer formation is very well seen on thin single pass samples after heat treatment (Fig. 14). It is important to note that even in the case of thin samples decarbonization develops exactly along the fine grain zone of normalising and inter critical temperatures [30].

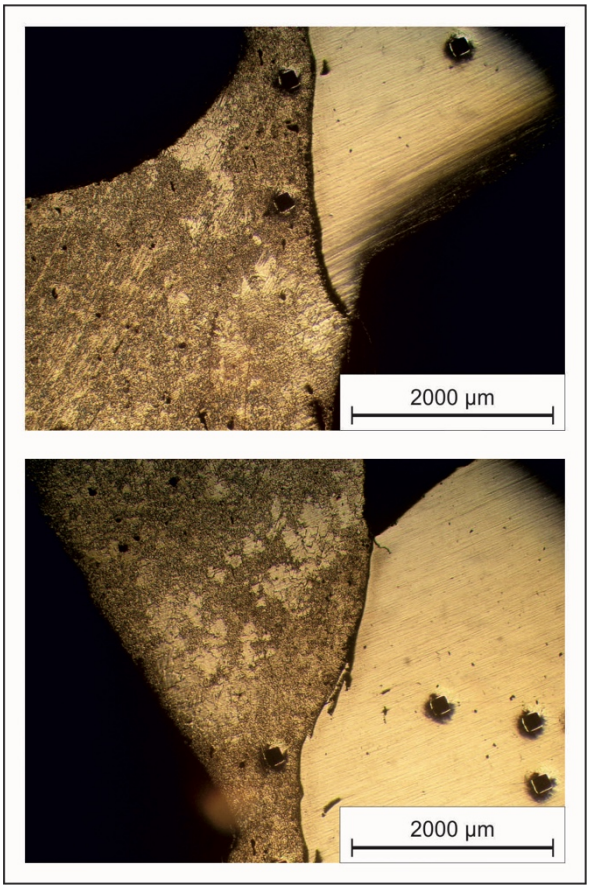

Fig. 14. Single pass weldments of 15Kh2M2FBS steel, welded with 9% Cr electrodes, after tempering at 740°C, 4 h

In the HAZ of the multi-pass welded joint (experiment No. 2) zones of refined grains/inter critical temperatures

from weld beads go out not only on the surface of base metal plates (Fig. 15a), but also on the fusion surface of the weld (Fig. 6, Fig. 7, Fig. 15b), which also has the role of diffusion intensifier due to the difference of chemical potential across the fusion line [30]. These zones form a frame for spreading ferrite interlayers (Fig. 15c), which help propagate ferrite towards the weld-adjacent zone in the HAZ during extended high-temperature exposure (Fig. 4b).

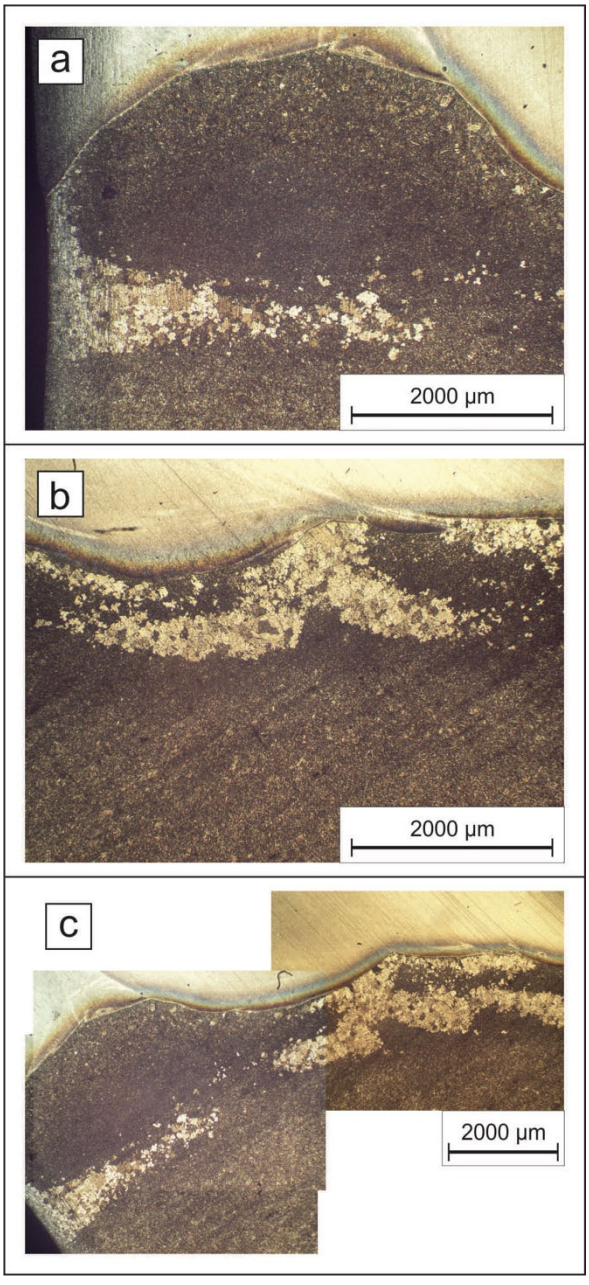

Fig. 15. Micrographs of the HAZ of welded joints made of 15Kh1M1F steel after tempering at 750°C, 6 h

In the experiment No. 2, after welding, a coarse-grained area of localised overheating occurs near the fusion line in the HAZ, in which the grain size differs from the grain size of the base metal and which, to a certain extent, affects the decarburisation rate at the initial stage of high-temperature exposure. It is assumed that under the influence of the same welding thermal cycle on the base metal with different initial grain sizes, the size of the formed grains in the coarse-grained HAZ will keep the same order as the size of the base metal grains: in the base metal with a large grain size the coarse-grained HAZ will have larger grain sizes than the coarse-grained HAZ in a fine-grained base metal. Therefore, in both 15Kh1M1F and 15Kh2M2FBS weldments after tempering, when comparing the average width of the decarburised layer in HAZ of sides with small and large initial grain size, the rule that the side with a larger base metal grain size has a smaller width of the layer, is preserved.

The difference in the kinetics of the formation of ferrite areas in the HAZ of 15Kh1M1F and 15Kh2M2FBS steels after tempering at 750°C, six h (Fig. 10) can be explained both by the differences in the chemical composition of the steels and by the assumption that during welding in the HAZ of 15Kh1M1F steel, a coarse-grained HAZ with a different grain size gradient dG/dx or dD/dx is formed (where G is the grain index, D is the average grain diameter, x is the direction perpendicular to the fusion surface) than in the HAZ of steel 15Kh2M2FBS. It is assumed that after exposure to 750°C for 12 h, the formation of ferrite areas begins to spread over the base metal, where the grain size index has established values unaffected by welding; therefore the dependence of the layer width on the grain size becomes linearly proportional.

The results of experiment 3 are explained by the fact that with increased heat input, a flatter thermal cycle causes a longer stay of the metal of the weld-adjacent zone at grain growth temperatures; the result is the formation of a wider area with coarse grains in the weld-adjacent zone, which should more strongly restrain the diffusion of carbon.

2.3. Suggested application

Deformation and fracture at high temperatures often occur along grain boundaries. This is explained by the fact that diffusion processes easily proceed along the grain boundaries containing many defects (vacancies, dislocations, etc.). When stresses are absent, diffusion displacements of boundary atoms are not directed. In the presence of even small stresses, these displacements of

atoms, especially at the grain boundaries, acquire a directed character, which contributes to the creep of the metal. In the creep process, one grain moves relative to another along the surface of their separation, the so-called sliding. Thus, if at low temperatures the grain boundaries slow down the movement of dislocations and strengthen the alloy, at high temperatures, on the contrary, they contribute to the accelerated softening of polycrystalline metals. Larger grains increase high-temperature strength, although ductility often decreases [33].

In this work, it was additionally shown that larger grain size of base metal leads to a decreased carbon diffusion rate in dissimilar welds.

The authors suggest that for various ferritic steels used in high-temperature dissimilar welded joints, it is possible to solve an optimisation problem – find the maximum grain size at which dissimilar welds will still meet the requirements for short-term mechanical properties specified in applicable standards. It is assumed that dissimilar joints made of such steels with the maximum acceptable grain size will have the highest values of long-term strength under conditions favourable for the development of type IIIa damage [15]. If this is the case, it may be appropriate to manufacture temperature high-temperature components (tubes, pipes, etc) with such grain size.

3. Conclusions

1. An increase in the grain size in the base metal of bainitic steels with 1.5...2% Cr leads to a decrease in the decarburisation rate in the HAZ of welded joints of these steels during tempering or high-temperature service.
2. 15Kh2M2FBS and 15Kh1M1F steels have different decarburization kinetics depending on the grain size index at the initial stage of tempering (after soaking for 6 hours at a temperature of 750°C); however, after a longer soak time of 12 hours, the dependence of the width of the decarburised layer on the grain size index becomes linear, proportional to the index.
3. An increase in the heat input of overlaying/welding leads to a decrease in the rate of decarburisation in the HAZ of welded joints of bainitic steels with 1.5...2% Cr during tempering and, probably, high-temperature operation.

In the conditions of conducted experiments using the manual arc welding process, it was established that the variation of the welding current or welding speed does not play a significant role in decarburisation, if the heat input at the same time remains unchanged.

References

[1] A. Di Gianfrancesco (ed), Materials for Ultra-Supercritical and Advanced Ultra-Supercritical Power Plants, Woodhead Publishing, Sawston, Cambridge, 2017. DOI: https://doi.org/10.1016/C2014-0-04826-5

[2] P. Mayr, C. Schlacher, J.A. Siefert, J.D. Parker, Microstructural features, mechanical properties and high temperature failures of ferritic to ferritic dissimilar welds, International Materials Reviews 64/1 (2019) 1-26. DOI: https://doi.org/10.1080/09506608.2017.1410943

[3] J.N. DuPont, Microstructural evolution and high temperature failure of ferritic to austenitic dissimilar welds, International Materials Reviews 57/4 (2012) 208-234. DOI: https://doi.org/10.1179/1743280412Y.0000000006

[4] T. Helander, H.C.M. Andersson, M. Oskarsson, Structural changes in 12-2,25 % Cr weldments - an experimental and theoretical approach, Materials at High Temperature 17/3 (2000) 389-396. DOI: https://doi.org/10.3184/096034000783640721

[5] Y. Zhao, J. Gong, X. Wang, W. Gao, Q. Li, Carbon diffusion in dissimilar joints between P91 and 12Cr1MoV steels welded by different consumables at high temperature, Materials at High Temperatures 32/6 (2015) 557-565. DOI: https://doi.org/10.1179/1878641315Y.0000000002

[6] R. Foret, B. Million, M. Svoboda, K. Stransky, Structural stability of dissimilar weld joints of steel P91, Science and Technology of Welding and Joining 6/6 (2001) 405-411. DOI: https://doi.org/10.1179/stw.2001.6.6.405

[7] K. Laha, S. Latha, K. Bhanu Sankara Rao, S.L. Mannan, D.H. Sastry, Comparison of creep behaviour of 2.25Cr–1Mo/9Cr–1Mo dissimilar weld joint with its base and weld metals, Materials Science and Technology 17/10 (2001) 1265-1272. DOI: https://doi.org/10.1179/026708301101509188

[8] W.K. Wang, J.X. Zhang, L.J. Zhang, Y. Liu, Q.B. Zhang, Microstructure and local mechanical properties of a dissimilar metal welded joint with buttering layer in steam turbine rotor, Materials Science and Engineering: A 747 (2019) 244-254. DOI: https://doi.org/10.1016/j.msea.2018.12.018

[9] A. Varma, R.K. Yadavalli, Failure analysis of a reheater tube dissimilar metal weld failure in a 500 MW power plant, Engineering Failure Analysis 118 (2020) 104851. DOI: https://doi.org/10.1016/j.engfailanal.2020.104851

[10] Q. Wu, Q. Xua, Y. Jianga, J. Gonga, Effect of carbon migration on mechanical properties of dissimilar weld joint, Engineering Failure Analysis 117 (2020) 104935. DOI: https://doi.org/10.1016/j.engfailanal.2020.104935
[11] Q. Wu, F. Lu, H. Cui, X. Liu, P. Wang, Y. Gao, Soft zone formation by carbon migration and its effect on the high-cycle fatigue in 9 % Cr–CrMoV dissimilar welded joint, Materials Letters 141 (2015) 242-244. DOI: https://doi.org/10.1016/j.matlet.2014.08.158
[12] W.-Ch. Zhang, M.-L. Zhu, K. Wang, F.-Zh. Xuan, Failure mechanisms and design of dissimilar welds of 9 %Cr and CrMoV steels up to very high cycle fatigue regime, International Journal of Fatigue 113 (2018) 367-376. DOI: https://doi.org/10.1016/j.ijfatigue.2018.04.032
[13] J. Yong, Zh. Zuo, G. Jianming, Carbon diffusion and its effect on high temperature creep life of Cr5Mo/A302 dissimilar welded joint, Acta Metallurgica Sinica 51/4 (2015) 393-399. DOI: https://doi.org/10.11900/0412.1961.2014.00435
[14] H. Cerjak, P. Mayr, Creep strength of welded joints of ferritic steels, in: F. Abe, T.-U. Kern, R. Viswanathan (eds), Creep-resistant steels, Woodhead Publishing, Sawston, Cambridge, 2008, 472-503. DOI: https://doi.org/10.1533/9781845694012.2.472
[15] S.J. Brett, Type IIIa cracking in 1/2CrMoV steam pipework systems, Science and Technology of Welding and Joining 9/1 (2004) 41-45. DOI: https://doi.org/10.1179/136217104225017134
[16] D. Jandová, J. Kasl, V. Kanta, Creep resistance of similar and dissimilar weld joints of P91 steel, Materials at High Temperatures 23/3-4 (2006) 165-170. DOI: https://doi.org/10.1179/mht.2006.010
[17] A. Kulkarni, D. K. Dwivedi, M. Vasudevan, Study of mechanism, microstructure and mechanical properties of activated flux TIG welded P91 Steel-P22 steel dissimilar metal joint, Materials Science and Engineering: A 731 (2018) 309-323. DOI: https://doi.org/10.1016/j.msea.2018.06.054
[18] J. Frei, B.T. Alexandrov, M. Rethmeier, Low heat input gas metal arc welding for dissimilar metal weld overlays part III: hydrogen-assisted cracking susceptibility, Welding in the World 63 (2019) 591-598. DOI: https://doi.org/10.1007/s40194-018-0674-7
[19] J.A. Fenske, I.M. Robertson, R. Ayer, M. Hukle, D. Lillig, B. Newbury, Microstructure and hydrogen-induced failure mechanisms in Fe and Ni alloy weldments, Metallurgical and Materials Transactions A 43 (2012) 3011-3022. DOI: https://doi.org/10.1007/s11661-012-1129-1
[20] M.L. Huang, L. Wang, Carbon migration in 5Cr-0.5Mo/21Cr-12Ni dissimilar metal welds, Metallurgical and Materials Transactions A 29 (1998) 3037-3046. DOI: https://doi.org/10.1007/s11661-998-0211-1
[21] A. Ul-Hamid, H.M. Tawancy, N.M. Abbas, Failure of weld joints between carbon steel pipe and 304 stainless steel elbows, Engineering Failure Analysis 12/2 (2005) 181-191. DOI: https://doi.org/10.1016/j.engfailanal.2004.07.003
[22] A. Kumar, S.M. Pandey, C. Pandey, Dissimilar weldments of ferritic/martensitic grade P92 steel and Inconel 617 alloy: Role of groove geometry on mechanical properties and residual stresses, Archives of Civil and Mechanical Engineering 23 (2023) 54. DOI: https://doi.org/10.1007/s43452-022-00592-5
[23] V. Bhanu, A. Gupta, C. Pandey, Investigation on joining P91 steel and Incoloy 800HT through gas tungsten arc welding for Advanced Ultra Super Critical (AUSC) power plants, Journal of Manufacturing Processes 80 (2022) 558-580. DOI: https://doi.org/10.1016/j.jmapro.2022.06.029
[24] G. Dak, C. Pandey, Study on effect of weld groove geometry on mechanical behavior and residual stresses variation in dissimilar welds of P92/SS304L steel for USC boilers, Archives of Civil and Mechanical Engineering 22 (2022) 140. DOI: https://doi.org/10.1007/s43452-022-00468-8
[25] C.D. Lundin, K.K. Khan, D. Yang, Effect of carbon migration in Cr-Mo weldments on metallurgical structure and mechanical properties, Welding Research Council Bulletin 407 (1995) 1-49.
[26] M.O. Nimko, Influence of welding parameters on decarburization in heat affected zone of dissimilar weldments after post weld heat treatment, Archives of Materials Science and Engineering 112/1 (2021) 23-31. DOI: https://doi.org/10.5604/01.3001.0015.5929
[27] L. Strilkova, Z. Kubon, V. Vodarek, Creep failure characteristics in P23/P91 dissimilar welds, Proceedings of the 19th International Metallurgical and Materials Conference "METAL 2010", Roznov pod Radhostem, Czech Republic, 2010, 65-70.
[28] V. Vodarek, Z. Kubon, R. Foret, S.V. Hainsworth, Microstructural evolution in P23/P91 heterogeneous welds during creep at 500–600°C, Proceedings of the IIW International Conference Safety and Reliability of Welded Components in Energy and Processing Industry, Graz, 2008, 217-223.
[29] ImageJ. Available from: https://imagej.nih.gov/ij/
[30] M.O. Nimko, V.Yu. Skulskyi, A.R. Gavryk, S.I. Moravetskyi, I.G. Osypenko, Structural inhomogeneity

in welded joints of heat-resistant steels of chromium-molybdenum-vanadium system with different chromium content, The Paton Welding Journal 10 (2021) 11-17.
DOI: https://doi.org/10.37434/tpwj2021.10.02
[31] J. Konieczny, Z. Rdzawski, P. Bańbura, B. Preficz, Influence of aging time and temperature on diffusion of alloyed copper, Journal of Achievements in Materials and Manufacturing Engineering 73/1 (2015) 27-35.
[32] H. Mehrer, Diffusion in Solids: Fundamentals, Methods, Materials, Diffusion-Controlled Processes, Springer Berlin, Heidelberg, 2007.
DOI: https://doi.org/10.1007/978-3-540-71488-0
[33] Y.M. Lakhtin, V.P. Leontieva, Material science, Third Edition, Mashinostroyéniye, Moscow, 1990 (in Russian).

© 2023 by the authors. Licensee International OCSCO World Press, Gliwice, Poland. This paper is an open-access paper distributed under the terms and conditions of the Creative Commons Attribution-NonCommercial-NoDerivatives 4.0 International (CC BY-NC-ND 4.0) license (https://creativecommons.org/licenses/by-nc-nd/4.0/deed.en).